Welding in the World (2022) 66:471–480
https://doi.org/10.1007/s40194-021-01234-9

RESEARCH PAPER

Laser beam welding setup for the coaxial combination of two laser beams to vary the intensity distribution

M. Möbus[1] · **P. Woizeschke**[1]

Received: 3 September 2021 / Accepted: 10 December 2021 / Published online: 10 January 2022

Abstract
Deep-penetration laser beam welding is highly dynamic and affected by many parameters. Several investigations using differently sized laser spots, spot-in-spot laser systems, and multi-focus optics show that the intensity distribution is one of the most influential parameters; however, the targeted lateral and axial intensity design remains a major challenge. Therefore, a laser processing optic has been developed that coaxially combines two separate laser sources/beams with different beam characteristics and a measuring beam for optical coherence tomography (OCT). In comparison to current commercial spot-in-spot laser systems, this setup not only makes it possible to independently vary the powers of the two laser beams but also their focal planes, thus facilitating the investigation into the influence of specific energy densities along the beam axis. First investigations show that the weld penetration depth increases with increasing intensities in deeper focal positions until the reduced intensity at the sample surface, due to the deep focal position, is no longer sufficient to form a stable keyhole, causing the penetration depth to drop sharply.

Keywords Laser beam welding · Laser intensity distribution · Beam shaping · Multi-focus

1 Introduction

The influence of the intensity distribution on the laser beam welding process is a widely investigated topic that, due to its complexity, still has open research questions. Numerous studies have been published on the keyhole behavior under certain intensity variations. For example, Weberpals and Dausinger analyzed the influence of the laser beam focusability [1], the inclination of the laser beam, and the variation of the focal plane on the keyhole angle and spatter formation [2]. Their results showed that laser beam welding with higher intensities facilitates a higher welding depth if the beam divergence angle is small enough. Furthermore, they showed that the decrease in the front keyhole wall inclination at negative focal positions increases the welding depth and decreases undesirable spatter formation.

Several investigations have aimed to determine the influence of shaped or multiple-spot intensities. Experiments with spot-in-spot laser technologies such as "BrightLine Weld" (TRUMPF GmbH + Co. KG) [3] or "Adjustable Ring Mode (ARM) Fiber Laser" (COHERENT, INC.) [4], which provide an inner core intensity and an outer ring intensity, revealed that the changed energy input decreases spatter formation, especially at higher welding speeds [3]. Punzel et al. investigated the influence of different intensity distributions on weld seam properties like penetration depth, seam width, and porosity and were able to achieve a reduction in porosity at certain intensity distributions [5]. They assumed that the reason for the reduced porosity is therefore a reduced vapor velocity due to an increased keyhole opening [5]. Nevertheless, these systems also have limitations because although the power distribution between the inner core and the outer ring can be set independently, they share the same focal plane.

Besides the findings of Weberpals and Dausinger, experiments with multi-focus optics also revealed the importance of the variation of the focal plane and intensity distribution along the beam axis. Volpp and Vollertsen showed that this

Recommended for publication by Commission IV - Power Beam Processes

✉ P. Woizeschke
woizeschke@bias.de

M. Möbus
moebus@bias.de

[1] BIAS - Bremer Institut für angewandte Strahltechnik GmbH, Klagenfurter Str. 5, 28359 Bremen, Germany

kind of axial beam shaping can be beneficial with respect to keeping the keyhole open and avoiding keyhole collapses and spatters [6]. In contrast to spot-in-spot laser technologies, the limitation of multi-focus optics is their fixed intensity distribution within the focal plane.

To vary both the focal plane and the intensity profile of several spots, various studies used the non-coaxial superposition of two separate laser intensities. Glumann et al. were presumably the first who merged two laser sources/beams non-coaxially to achieve higher total power [7]. Nagel et al. used two different laser sources and optics that set the different sized laser beams at an angle of 45° to each other ("off-axis" non-coaxial beam combination) and showed a decreasing amount of material loss during welding due to keyhole stabilization as a result of the superposition [8].

The literature shows the potential of a freely selectable intensity distribution, but current systems have limitations. Therefore, this study develops a laser processing optic that coaxially combines two separate laser sources/beams with different beam characteristics, allowing the total intensity distribution along and perpendicular to the beam axis to be freely adjusted by varying the power distribution between both lasers and their respective focal positions independently. The objective of the following experimental work is to validate the function of the setup and to show the preliminary results for the variation of the intensity distribution.

2 Experimental

2.1 Processing setup

The developed laser processing setup is shown in Fig. 1 and schematically presented in Fig. 2. Within the setup, two dichroic mirrors with specific coatings allowing a narrow band transition combine the separate beams which can be emitted by any laser source providing wavelengths of 1030 nm (processing laser source no. 1), 1070 nm (processing laser source no. 2), and less or equal than 1030 nm (OCT—optical coherence tomography). Beam combiner no. 1 reflects more than 99.9% of radiation with a 1030 nm wavelength, irradiated by processing laser source no. 1, and transmits more than 95% of the radiation with a wavelength between 800 and 900 nm, which is used by the OCT system Laser Depth Dynamics LD-600 (Laser Depth Dynamics Inc.; nowadays part of IPG Photonics Corporation). Beam combiner no. 2 coaxially combines the beams of the OCT system and the processing laser source no. 1 with the beam of the processing laser source no. 2 by reflecting 99.9% of the radiation with a wavelength of 1070 nm (processing laser beam no. 2) and transmitting more than 95% of radiation with a wavelength of 1030 nm. Due to the high complexity, the coating can only be produced so that merely 85% of the OCT beam radiation is transmitted on

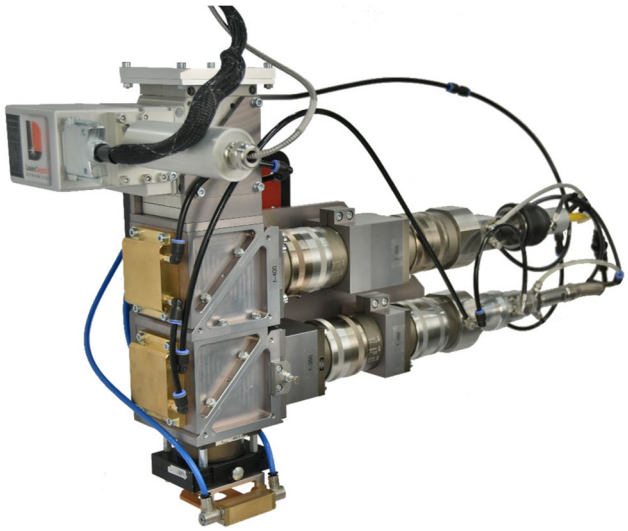

Fig. 1 Developed processing setup

average, leading to an undesirable signal in the measuring due to the reflection; this needs to be considered or filtered out afterwards. To determine the maximum possible total laser power, tests with up to 5 kW have been safely carried out so far. It is expected that higher powers are possible.

Both the collimating and focusing lenses are positioned before the beams merge. Due to the fact that the lengths of the beam paths differ by 50 mm and the focal length of the upper focusing lense was also chosen 50 mm longer, both beams share the same initial focal plane. The position of all lenses can be moved within the beam path. This allows for the adjustment of the focal plane in the z-direction and of the beam properties, such as focus diameter and Rayleigh length, independently of each other. The maximum adjustable distance between the two foci in the z direction is 15 mm when only the focusing lenses are shifted and 50 mm when the collimating lenses are additionally shifted (which leads to a change in the beam profiles depending on the used laser source), with an accuracy of ± 50 µm. In addition to the z direction, the focal planes can also be adjusted relative to each other in the y- and x-directions. For this purpose, it is possible to shift the upper beam path in the z-direction, which results in a shift of maximum ± 3 mm of the focal plane in the x-direction, and the lower beam path in the y-direction, which results in a shift of maximum ± 3 mm of the focal plane in the y-direction.

2.2 Experimental setup

Mild steel S235JRC was used for the bead-on-plate welding experiments. The chemical composition is given in Table 1. The dimensions of the specimens as well as the positions of

the weld seams and the cross-sections for the metallographic analyses can be found in Fig. 3.

The experimental setup can be found in Fig. 2. The specimen was placed on a moving table that provided a constant welding speed of 2 m/min to produce a bead-on-plate seam length of 50 mm. The irradiation angle of the processing setup was tilted by 5° to the vertical orientation in the welding direction. Argon was used as a shielding gas with a flow rate of 7 l/min.

The experiments were carried out using a TruDisk12002 laser source (TRUMPF GmbH + Co. KG) as processing laser source no. 1 and a YLR-8000S laser source (IPG Photonics Corporation) as processing laser source no. 2. The settings and properties of the two laser sources are summarized in Table 2. The intensity profiles in the focal plane for both laser beams as well as their combinations with different power distributions and focal distances, measured by the HighPowerMSM (Primes GmbH), can be seen in Fig. 4.

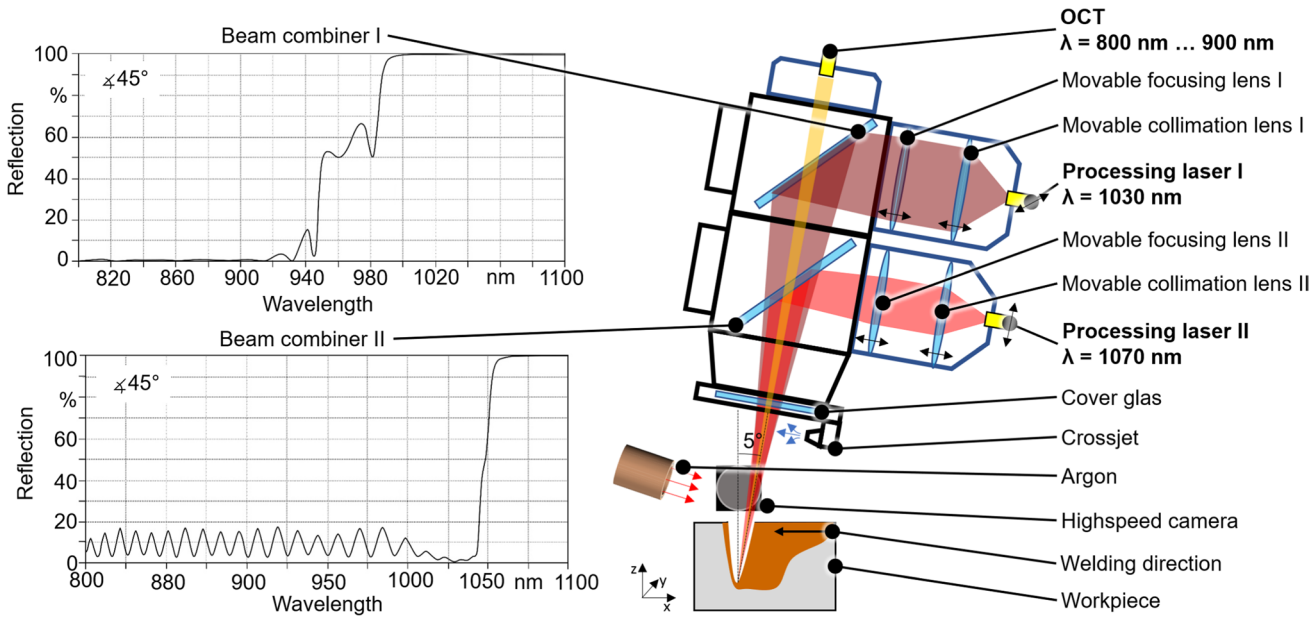

Fig. 2 Schematical laser processing and experimental setup

Table 1 Chemical composition of S235JRC according to the datasheet [9]

Fe	Mn	Cu	Si	Cr	Ni	C
Bal	0.52	0.23	0.20	0.16	0.13	0.08

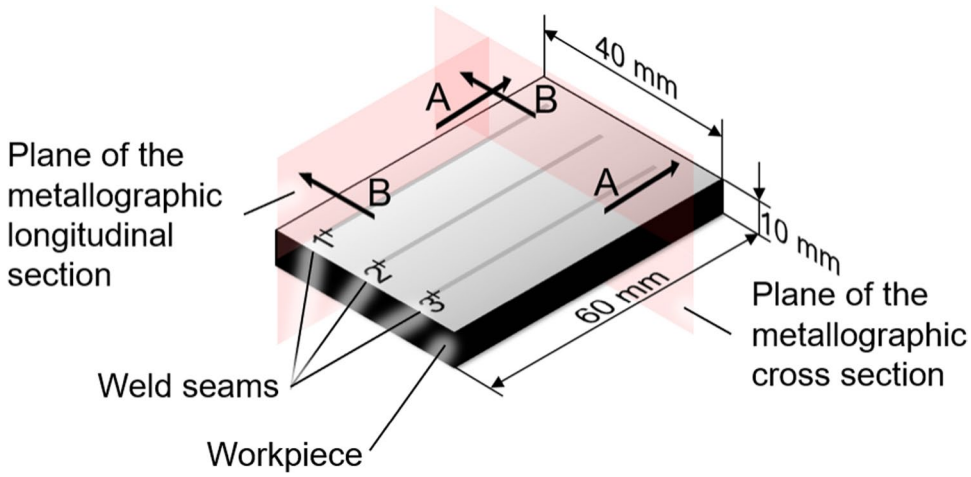

Fig. 3 Dimensions of the specimen

Table 2 Settings of the laser beams

Manufacture	Processing laser source I Trumpf TruDisk12002	Processing laser source II IPG-YLR-8000S
Wavelength λ	1030 nm	1070 nm
Fiber diameter d_{Fi}	200 µm	100 µm
Focal length of the collimating lens	200 mm	200 mm
Focal length of the focusing lens	400 mm	350 mm
Focus diameter	390 µm	180 µm
Laser power	0 kW … 3 kW	0 kW … 3 kW
Angle of incidence	5°	5°
Focal plane F_P	0 mm, – 2 mm, – 4 mm, – 6 mm	0 mm, – 2 mm, – 4 mm, – 6 mm
M^2	25.1	14.6
Rayleigh length	4.2 mm	1.6 mm

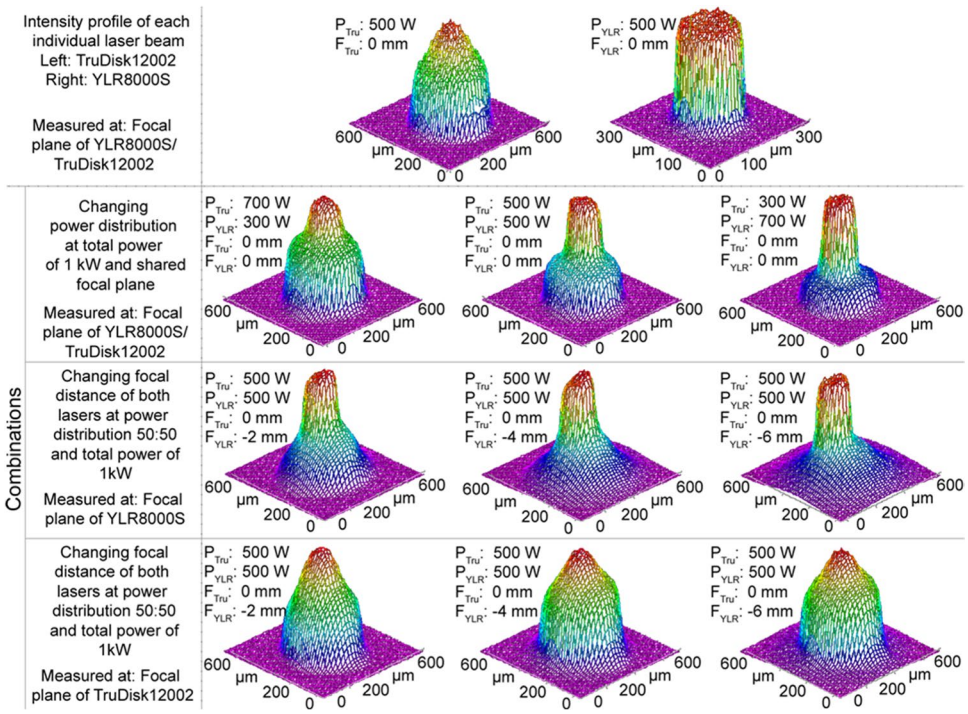

Fig. 4 Measured intensity profiles of the used laser beams and their combinations with different power distributions and focal distances

During the entire series of tests, the total power was kept constant at 3 kW, but the power distribution between the laser beams and their focal planes was varied full factorially, whereby deep penetration welding could always be achieved. The factor levels of the power distribution were set in 20% steps from 100% TruDisk12002 to 100% YLR 8000S, and the factor levels of the focal plane were 0 mm, -2 mm, -4 mm and -6 mm. Each parameter combination was repeated three times.

The welding process was observed via high-speed imaging using a Phantom VEO 410L (Vision Research, Wayne, NJ, USA) high-speed camera in combination with a Cavilux HF illumination laser (Cavitar Ltd, Tampere, Finland) operating at a wavelength of 810 nm with a narrow band-pass filter with a central wavelength of 810 nm with a full width at the half-maximum of 12 nm. The high-speed videos were recorded at a framerate of 20 kHz and were used for spatter tracking of the samples with the factor levels of the focal plane at 0 mm, -2 mm, -4 mm and -6 mm with a MATLAB based tracking algorithm that recorded the overall average spatter amount per sample by multiplying the average spatter size and the average number of spatters.

Metallographic cross-sections (A-A, cf. Figure 3) were taken to measure the average penetration depth as well as the standard deviation. One longitudinal section (B-B, cf. Figure 3) per sample was taken to analyze the seam porosity.

To evaluate the data obtained from the statistical experimental design, MATLAB-based regression models were fitted and hypothesis significance tests were performed. The latter helped to find the statistically significant influence

coefficients to a significance level of 5% by outputting the *p*-value, which is the probability that a larger value of the test statistic would occur if the factor in question had zero effect on the mean or variance in question [10]. If the *p*-value of a coefficient was less than the significance level, the coefficient was considered significant.

3 Results

3.1 Intensity profile

Figure 4 shows the measured intensity profiles in the focal plane for both laser beams as well as their combinations with different power distributions and focal distances. It can be seen that the intensity distribution within the measured plane changes when changing the power distribution and the focal distance. Especially when comparing the changes in the intensity distribution due to the variation of the power distribution, it can be seen that the intensities of each separate laser beam add up when combined. By increasing the laser power of the TruDisk12002, the pedestal-shaped intensity distribution around the center rises. In reality, the center, which is mainly the intensity distribution of the YLR-8000S, would simultaneously decrease to a lower value, but this is not visible here because the software scales every intensity distribution to 100% of the z-axis. By comparing the changes in the intensity distribution due to the variation of the focal distance, the same addition effect can be observed. Within the focal plane of the YLR-8000S the center intensity stays the same when increasing the focal distance between both laser beams, while the outer form widens because of the increasing spot diameter of the TruDisk12002 within this plane. Within the focal plane of the TruDisk12002, the effect is less visible because the bigger spot diameter of the TruDisk12002 covers the influence of the widening spot diameter of the YLR-8000S within this plane.

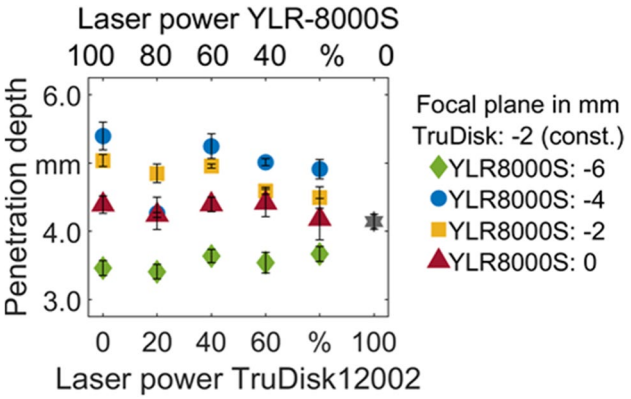

Fig. 6 Penetration depth (cross-section measurements) against power distribution with a constant focal plane at -2 mm of the TruDisk12002 and a varying focal plane of the YLR 8000S

3.2 Penetration depth

Figure 5 displays the penetration depth against the varying power distribution between both laser beams for a constant focal plane of the TruDisk12002 laser beam at 0 mm and the changing focal plane of the YLR-8000S laser beam. As can be seen, deeper focal planes of the YLR-8000S from 0 mm to -4 mm lead to deeper penetration depths over all power distributions. One exception can be observed at the focal plane – 6 mm, where the welding depth shows its lowest values over the entire power distribution. Apart from this exception, the penetration depth constantly increases from 100% TruDisk12002 to 100% YLR-8000S for the focal plane variations of YLR-8000S from 0 mm to -4 mm.

Figures 6, 7, and 8 display the penetration depth over the varying power distribution for changing focal planes of the

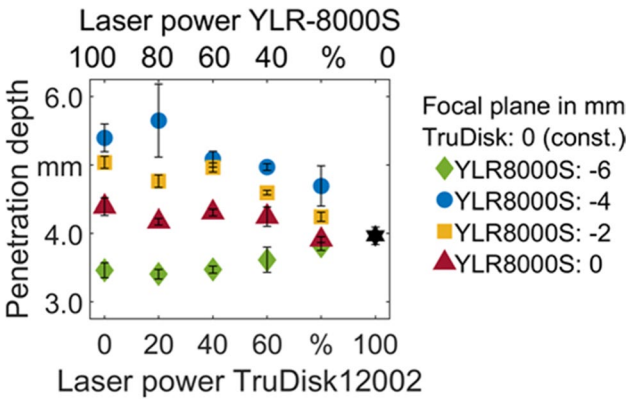

Fig. 5 Penetration depth (cross-section measurements) against power distribution with a constant focal plane at 0 mm of the TruDisk12002 and a varying focal plane of the YLR-8000S

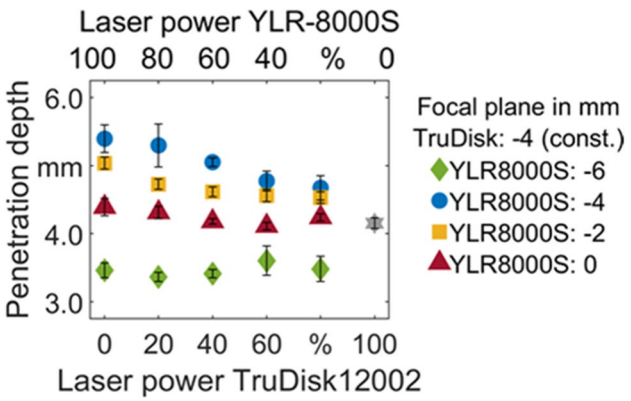

Fig. 7 Penetration depth (cross-section measurements) against power distribution with a constant focal plane at -4 mm of the TruDisk12002 and a varying focal plane of the YLR-8000S

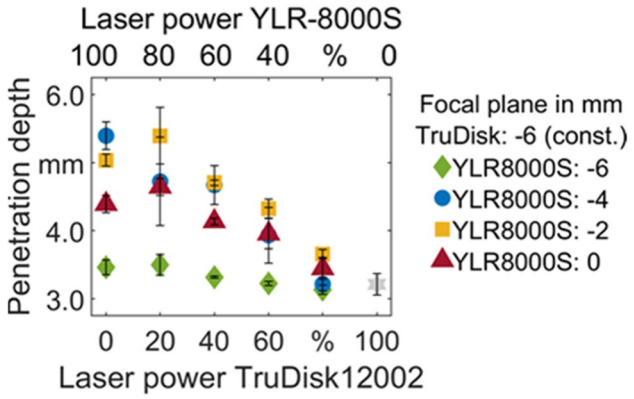

Fig. 8 Penetration depth (cross-section measurements) against power distribution with a constant focal plane at -6 mm of the TruDisk12002 and a varying focal plane of the YLR 8000S

Table 3 Results of the hypothesis testing for penetration depth

Coefficient	*p*-value
Power distribution	0.0327
Focal plane TruDisk12002	0.0687
Focal plane YLR-8000S	0.0025

YLR-8000S and constant focal planes of the TruDisk12002 at -2 mm, -4 mm, and -6 mm, respectively. Figure 5 also shows the increasing average penetration depths with deeper focal planes and rising power of the YLR-8000S, although the average standard deviation increases slightly from -2 mm to -4 mm (focal planes of YLR-8000S).

Furthermore, it becomes clear that although the focal plane of the TruDisk12002 varies between the results given in Figs. 5, 6, 7, and 8, the penetration depth barely changes.

The results of the hypothesis testing, listed in Table 3, show that the power distribution and the focal plane of the YLR 8000S must be considered as significant coefficients that influence the penetration depth. The focal plane of the TruDisk12002 laser beam is not assessed as a significant coefficient influencing the penetration depth.

The observations mentioned above can also be detected in the metallographic cross sections, displayed in Fig. 9. It can be seen that the penetration depth changes only slightly with variation of the focal position of the TruDisk12002 (left side), whereas it changes strongly with variation of the focal position of the YLR-8000S (right side). One striking feature is noticeable. For the focal positions F_{Tru}: 0 mm, F_{YLR}: -4 mm and the power distribution P_{Tru}: 20%, P_{YLR}: 80% it can be seen that the shape of the seam first becomes narrower, widens again in the depth of approximately 2.5 mm and then becomes narrower again.

3.3 Spatter amount

Figure 10 shows the spatter amount against the varying power distribution between both laser beams for a constant

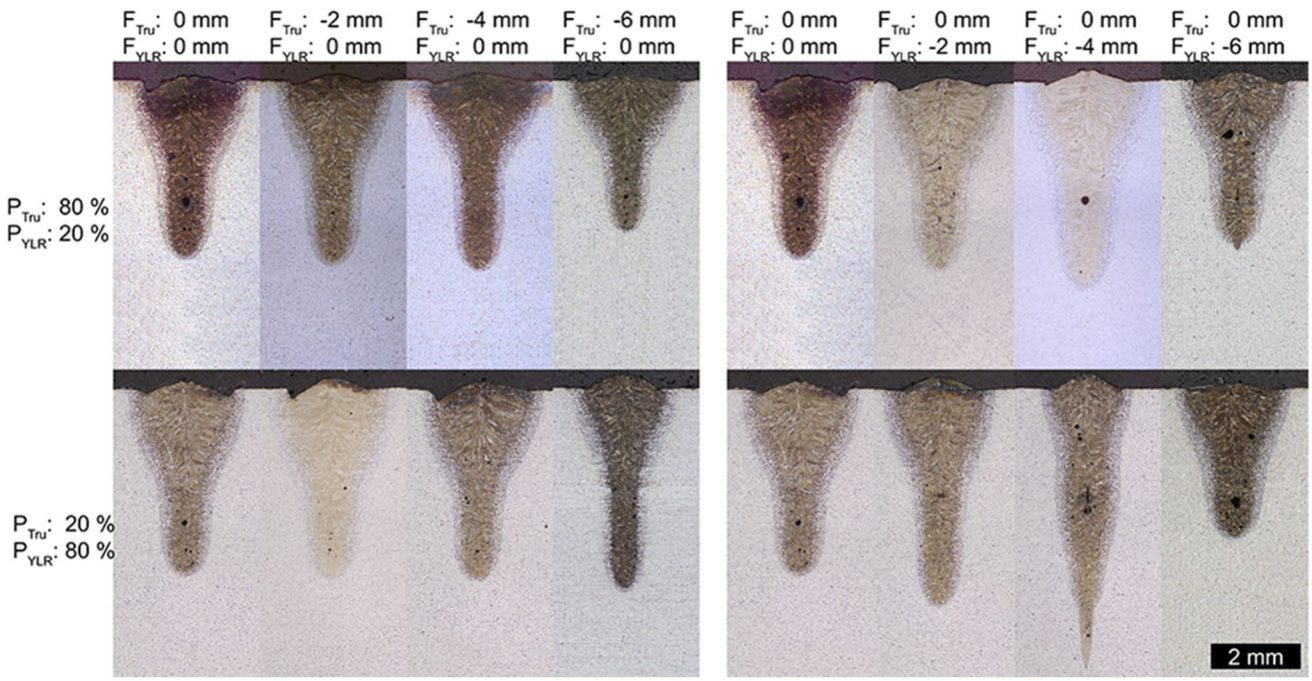

Fig. 9 Metallographic cross sections with different power distributions P (at constant overall power of 3 kW) and different focal positions F of both laser beams

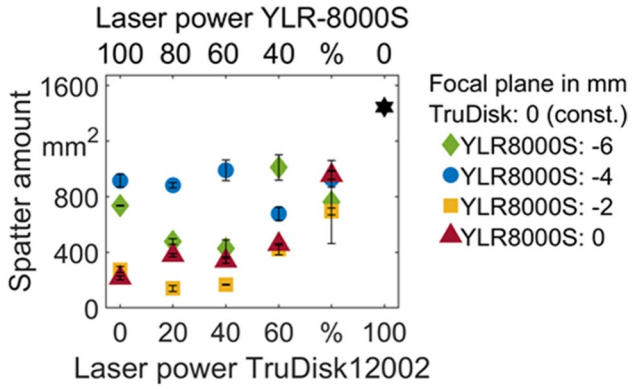

Fig. 10 Spatter amount (high-speed imaging) against power distribution with a constant focal plane at 0 mm of the TruDisk12002 and a varying focal plane of the YLR 8000S

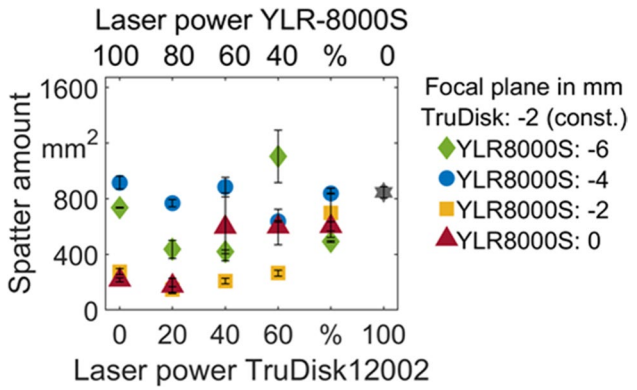

Fig. 11 Spatter amount (high-speed imaging) against power distribution with a constant focal plane at -2 mm of the TruDisk12002 and a varying focal plane of the YLR 8000S

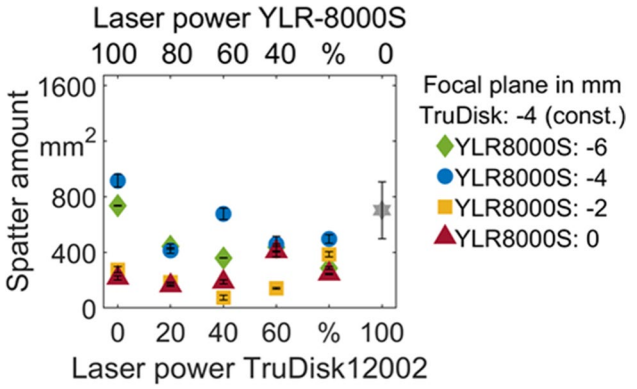

Fig. 12 Spatter amount (high-speed imaging) against power distribution with a constant focal plane at -4 mm of the TruDisk12002 and a varying focal plane of the YLR 8000S

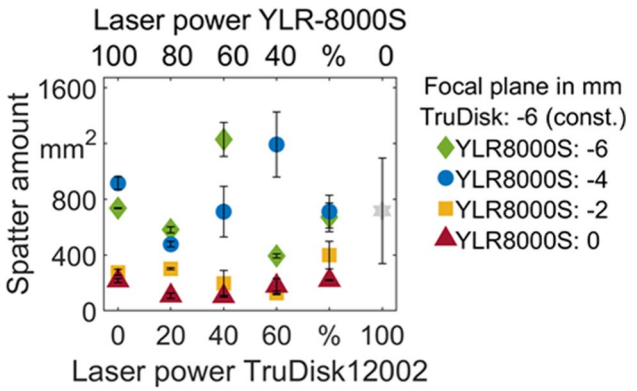

Fig. 13 Spatter amount (high-speed imaging) against power distribution with a constant focal plane at -6 mm of the TruDisk12002 and a varying focal plane of the YLR 8000S

focal plane of the TruDisk12002 at 0 mm and changing focal plane of the YLR-8000S. Across almost all power distributions, a focal plane of the YLR-8000S at -2 mm results in a minimum spatter amount. For the focal plane of the YLR-8000S at 0 mm, the rising laser power of the TruDisk12002 increases the spatter amount, while for -2 mm a minimum can be observed at 20% TruDisk12002, and for -4 mm the spatter amount fluctuates around 800 mm^2 and increases only for 100% TruDisk12002.

Comparing the spatter amount of the tests with a focal plane of the TruDisk12002 at 0 mm in Fig. 10 with focal planes at -2 mm (Fig. 11), -4 mm (Fig. 12) and − 6 mm (Fig. 13), commonalities are noticeable. In all of the other figures, the minimum spatter amount is also reached with a focal plane of the YLR-8000S at -2 mm respectively 0 mm. Furthermore, with the focal plane of the YLR-8000S at 0 mm and -2 mm, the spatter amount presents a minimum between 20 and 40% TruDisk12002 and increases significantly for laser power values of the TruDisk12002 over 60%, while at -4 mm and -6 mm, the power distribution shows no definite effect on the spatter amount. A focal plane of the TruDisk12002 deeper than 0 mm reduces the spatter amount when the power distribution is set at 100% TruDisk12002.

Table 4 Results of the hypothesis testing for the spatter amount

Coefficient	*p*-value
Power distribution	0.0159
Focal plane TruDisk12002	0.0297
Focal plane YLR-8000S	0.0000

The results of the associated hypothesis test, listed in Table 4, support that all coefficients must be considered as significant factors that influence the spatter amount.

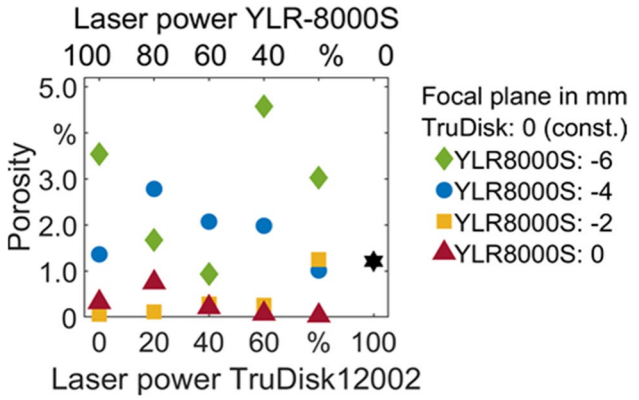

Fig. 14 Porosity (longitudinal section) against power distribution with a constant focal plane at 0 mm of the TruDisk12002 and a varying focal plane of the YLR 8000S

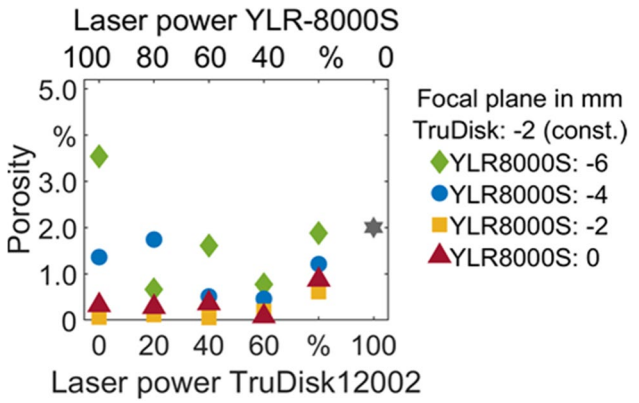

Fig. 15 Porosity (longitudinal section) against power distribution with a constant focal plane at -2 mm of the TruDisk12002 and a varying focal plane of the YLR 8000S

3.4 Porosity

The porosities over the varying power distribution between both laser beams for the focal planes of the TruDisk12002 and the YLR-8000S from 0 mm to -6 mm are shown in Figs. 14, 15, 16 and 17. There is not much difference in the expression of the data points when comparing these four figures. This illustrates that the focal plane of the TruDisk12002 does not have a great influence on the porosity. Furthermore, the power distribution also has no great influence on the porosity, as the data points present no trends from 100% YLR-8000S to 100% TruDisk12002. For the focal plane of the YLR-8000S at 0 mm and -2 mm, it can be seen that the porosity is reduced in comparison to -4 mm and -6 mm.

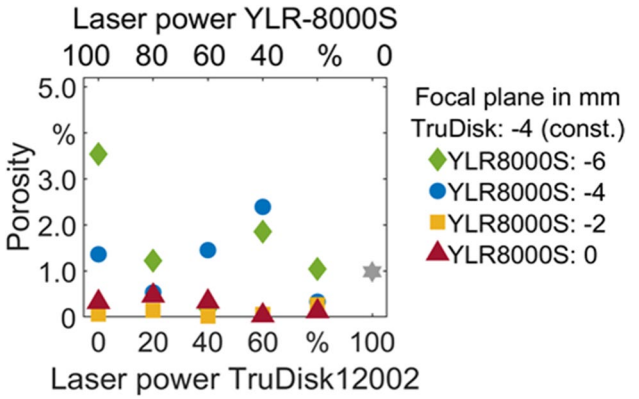

Fig. 16 Porosity (longitudinal section) against power distribution with a constant focal plane at -4 mm of the TruDisk12002 and a varying focal plane of the YLR 8000S

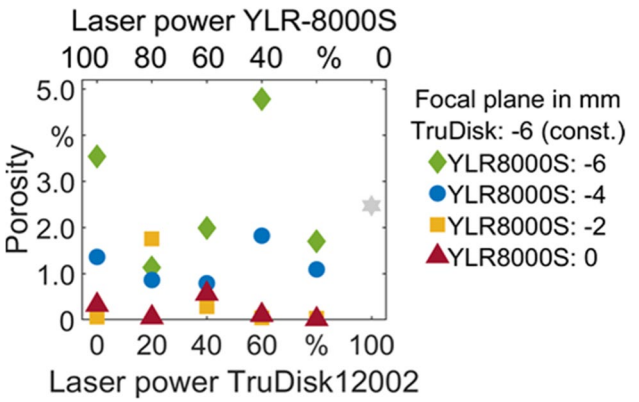

Fig. 17 Porosity (longitudinal section) against power distribution with a constant focal plane at -6 mm of the TruDisk12002 and a varying focal plane of the YLR 8000S

Table 5 Results of the hypothesis testing for porosity

Coefficient	*p*-value
Power distribution	0.5598
Focal plane TruDisk12002	0.3749
Focal plane YLR-8000S	0.0000

The results of the associated hypothesis testing in Table 5 underline the observations. The only significant coefficient is the focal plane of the YLR 8000S.

4 Discussion

The experiments have revealed that the penetration depth increases with rising intensity and deeper focal positioning from 0 mm to -4 mm of the YLR-8000S laser beam. The

results are in good agreement with the literature stating that higher intensities lead to increased penetration depth [11]. This is because, although the total laser power remains constant over the entire series of tests, the intensity multiplies when changing the power distribution from 100% TruDisk12002 to 100% YLR-8000S due to the fact that the laser beam spot diameter of the YLR-8000S (180 µm) is about half as small as the spot diameter of the TruDisk12002 (390 µm), resulting in deeper keyholes.

The increasing penetration depth with deepening focal planes from 0 mm to − 4 mm, as shown for the YLR-8000S, is an often-described effect [11]. When changing the focal plane of the YLR-8000S from -4 mm to -6 mm, the penetration depth sharply decreases. This can be explained by the increasing beam diameter on the sample surface while maintaining the same total power and thus the decreasing intensity on the sample surface, which is no longer sufficient to provide a (stable) keyhole. This statement is supported by the results for the standard deviation of the penetration depth, the spatter amount and the porosity. Based on the results shown in Fig. 5 to Fig. 17, it is apparent that the process stability decreases by varying the focal plane of YLR-8000S from -2 mm to -4 mm because the spatter amount and the porosity increases in all cases. Furthermore, a trend can also be seen in the standard deviation of the penetration depth, as mentioned in 3.2. A reason for the largely absent effect of the focal plane of the TruDisk12002 could be its Rayleigh length of 4.2 mm. The already smaller intensity distribution in comparison to the YLR-8000S due to the bigger spot diameter, changes to a comparatively lower extent when varying the focal position from 0 mm to -4 mm, probably resulting in the small differences for most of the measured values. Only for the focal position F_{Tru}: -6 mm, which is above the Rayleigh length and significantly deeper than the present penetration depth, and with increased power percentage of the TruDisk12002, a change in the form of a decreasing penetration depth can be detected (cf. Figure 9).

Based on the cross-section with the focal positions F_{Tru}: 0 mm, F_{YLR}: -4 mm and the power distribution P_{Tru}: 20%, P_{YLR}: 80%, displayed in Fig. 9, which first becomes narrower, widens again in the depth of approximately 2.5 mm and then becomes narrower again, it can be concluded that the deeper focal position of the YLR-8000S actually leads to a shift of the effective intensity also deeper into the sample. This effect can also be observed weaker for the power distributions P_{Tru}: 40%, P_{YLR}: 60% and P_{Tru}: 60%, P_{YLR}: 40%.

5 Summary

This paper presents a laser beam welding setup for the coaxial combination of two laser sources. Furthermore, the influence of specific intensity distributions along the beam axis was studied. The results suggest that higher intensities in deeper focal positions increase the weld penetration depth to the focal position where the intensity at the sample surface is no longer sufficient to form a stable deep keyhole and until then when the focal plane is significantly below the actual current penetration depth, causing the penetration depth to drop sharply.

Acknowledgements The authors gratefully acknowledge funding from the German Research Foundation (Deutsche Forschungsgemeinschaft DFG, project numbers 423364400 and 331150978). Many thanks are due to Mr. Ronald Pordzik for the development and programming of the spatter tracking algorithm.

Funding Open Access funding enabled and organized by Projekt DEAL. The study was funded by the German Research Foundation (Deutsche Forschungsgemeinschaft DFG, project numbers 423364400 and 331150978).

Declarations

Conflict of interest The authors declare no competing interests.

References

1. Weberpals J, Dausinger F, Göbel G, Brenner B (2006) The role of strong focusability on the welding process. ICALEO® 2006: 25th International Congress on Laser Materials Processing and Laser Microfabrication; October 30–November 2, 2006; Scottsdale, Arizona, USA; In: International Congress on Applications of Lasers & Electro-Optics; Laser Institute of America (2006) 905
2. Weberpals J, Dausinger F (2008) Fundamental understanding of spatter behavior at laser welding of steel. ICALEO® 2008: 27th International Congress on Laser Materials Processing, Laser Microprocessing and Nanomanufacturing; October 20–23, 2008; Temecula, California, USA; In: International Congress on Applications of Lasers & Electro-Optics; Laser Institute of America (2008) 704
3. Haug P, Weidegang S, Seebach J, Speker N, Hesse T, Bisch S (2019) Beam shaping BrightLine Weld – latest application results. In: Lasers in Manufacturing Conference
4. Wang L, Mohammadpour M, Gao X, Lavoie J-P, Kleine K, Kong F, Kovacevic R (2021) Adjustable Ring Mode (ARM) laser welding of stainless steels. Opt Lasers Eng 137:106360
5. Punzel E, Hugger F, Dinkelbach T, Bürger A (2020) Influence of power distribution on weld seam quality and geometry in laser beam welding of aluminum alloys. Procedia CIRP 94:601–604
6. Volpp J, Vollertsen F (2019) Impact of multi-focus beam shaping on the process stability. Opt Laser Technol 112:278–283

7. Glumann C, Rapp J, Dausinger F, Hügel H (1993) Welding with combination of two CO2-lasers - advantages in processing and quality. ICALEO® '93: Proceedings of the Laser Materials Processing Conference; October 24–28, 1993; Orlando, Florida, USA; In: International Congress on Applications of Lasers & Electro-Optics; Laser Institute of America: 672-681
8. Nagel F, Brömme L, Bergmann JP (2019) Effects of two superimposed laser beams on spatter formation during laser welding of high alloyed steel. J Laser Appl 31(2):22005
9. Andernach & Bleck GmbH &Co.KG (2020) Abnahmeprüfzeugnis EN10204 - 3.1 - S235JRC
10. Allen TT (2006) Introduction to engineering statistics and six sigma - statistical quality control and design of experiments and systems 2 Springer-Verlag London Limited; London
11. Weberpals J-P, Krueger P, Berger P, Graf T (2011) Understanding the influence of the focal position in laser welding on spatter reduction. ICALEO® 2011: 30th International Congress on Laser Materials Processing, Laser Microprocessing and Nanomanufacturing; October 23–27, 2011; Orlando, Florida, USA; In: International Congress on Applications of Lasers & Electro-Optics; Laser Institute of America (2011) 159-168